# CHAPTER 1

# SYMMETRY AND PATTERN FORMATION ON THE VISUAL CORTEX

Martin Golubitsky*, LieJune Shiau†, and Andrei Török*

* *Department of Mathematics, University of Houston, Houston, TX 77204-3008, USA*

† *Department of Mathematics, University of Houston – Clear Lake, Houston, TX 77058, USA*

Mathematical studies of drug induced geometric visual hallucinations include three components: a model that abstracts the structure of the primary visual cortex V1; a mathematical procedure for finding geometric patterns as solutions to the cortical models; and a method for interpreting these patterns as visual hallucinations. In this note we survey the symmetry based ways in which geometric visual hallucinations have been modelled. Ermentrout and Cowan model the activity of neurons in the primary visual cortex. Bressloff, Cowan, Golubitsky, Thomas, and Wiener include the orientation tuning of neurons in V1 and assume that lateral connections in V1 are *anisotropic*. Golubitsky, Shiau, and Török assume that lateral connections are *isotropic* and then consider the effect of perturbing the lateral couplings to be weakly anisotropic.

These models all have planar Euclidean $\mathbf{E}(2)$ symmetry. Solutions are assumed to be spatially periodic and patterns are formed by symmetry-breaking bifurcations from a spatially uniform state. In the Ermentrout-Cowan model $\mathbf{E}(2)$ acts in its standard representation on $\mathbf{R}^2$, whereas in the Bressloff *et al.* model $\mathbf{E}(2)$ acts on $\mathbf{R}^2 \times \mathbf{S}^1$ via the *shift-twist* action. Isotropic coupling introduces an additional $\mathbf{S}^1$ symmetry, and weak anisotropy is then thought of as forced symmetry-breaking from $\mathbf{E}(2)\dot{+}\mathbf{S}^1$ to $\mathbf{E}(2)$ in its shift-twist action. We outline the way symmetry appears in bifurcations in these different models.

## 1. Introduction to Geometric Visual Hallucinations

When describing drug induced geometric visual hallucinations Klüver [17] states on p. 71: "We wish to stress merely one point, namely, that under diverse conditions the visual system responds in terms of a limited number of form constants." Klüver then classified geometric visual hallucinations into four groups or *form constants*: honeycombs, cobwebs, funnels and tunnels,

and spirals. See Figure 1.

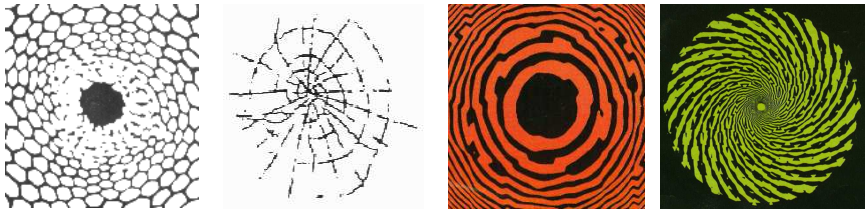

(a) (b) (c) (d)

Fig. 1. (a) Honeycomb by marihuana; [8] (b) cobweb petroglyph; [20] (c) tunnel [21], (d) spiral by LSD [21].

Ermentrout and Cowan [10] pioneered an approach to the mathematical study of geometric patterns produced in drug induced hallucinations. They assumed that the drug uniformly stimulates an inactive cortex and produces, by spontaneous symmetry-breaking, a patterned activity state. The mind then interprets the pattern as a visual image — namely the visual image that would produce the same pattern of activity on the primary visual cortex V1.[a] The Ermentrout-Cowan analysis assumes that a differential equation governs the symmetry-breaking transition from an inactive to an active cortex and then studies abstractly the transition using standard pattern formation arguments developed for reaction-diffusion equations. Their cortical patterns are obtained by thresholding (points where the solution is greater than some threshold are colored black, whereas all other points are colored white). These cortical patterns are then transformed to retinal patterns using the inverse of the retino-cortical map described in (4), and these retinal patterns are similar to some of the geometric patterns of visual hallucinations, namely, funnels and spirals.

In this note we survey recent work of Bressloff, Cowan, Golubitsky, Thomas, and Wiener [4–6] and Golubitsky, Shiau, and Török [13] who refine the Ermentrout-Cowan model to include more of the structure of V1. Neurons in V1 are known to be sensitive to orientations in the visual field[b] and it is mathematically reasonable to assign an orientation preference to

[a]The *primary visual cortex* is the area of the visual cortex that receives electrical signals directly from the retina.

[b]Experiments show that most V1 cells signal the local orientation of a contrast edge or bar; these neurons are tuned to a particular local orientation. See [1,3,12,16] and [5] for further discussion.

each neuron in V1. Hubel and Wiesel [16] introduced the notion of a *hypercolumn* — a region in V1 containing for each orientation at a single point in the visual field (a mathematical idealization) a neuron sensitive to that orientation.

Bressloff *et al.* [5] studied the geometric patterns of drug induced hallucinations by including orientation sensitivity. As before, the drug stimulation is assumed to induce spontaneous symmetry-breaking, and the analysis is local in the sense of bifurcation theory. There is one major difference between the approaches in [5] and [10]. Ignoring lateral boundaries Ermentrout and Cowan [10] idealize the cortex as a plane, whereas Bressloff *et al.* [5] take into account the orientation tuning of cortical neurons and idealize the cortex as $\mathbf{R}^2 \times \mathbf{S}^1$. This approach recovers thin line hallucinations such as cobwebs and honeycombs, in addition to the threshold patterns found in the Ermentrout-Cowan theory.

There are two types of connections between neurons in V1: local and lateral. Experimental evidence suggests that neurons within a hypercolumn are all-to-all connected, whereas neurons in different hypercolumns are connected in a very structured way. This structured lateral coupling is called *anisotropic*, and it is the bifurcation theory associated with anisotropic coupling that is studied in Bressloff *et al.* [4, 5].

Golubitsky, Shiau, and Török [13] study generic bifurcations when lateral coupling is weakly anisotropic. First, they study bifurcations in models that are isotropic showing that these transitions lead naturally to a richer set of planforms than is found in [4, 5] and, in particular, to time-periodic states. (Isotropic models have an extra $\mathbf{S}^1$ symmetry and have been studied by Wolf and Geisel [24] as a model for the development of anisotropic lateral coupling.) There are three types of time dependent solutions: slowly *rotating* spiral and funnel shaped retinal images; *tunneling* images where the retinal image appears to rush into or spiral into the center of the visual field; and *pulsating* images where the spatial pattern of the solution changes periodically in time. Movies of these states may be found in [13]. Such images have been reported in the psychophysics literature, see Klüver [17], p. 24. (Note that near death experiences are sometimes described as traveling down a tunnel toward a central area.) Second, they consider weak anisotropy as forced symmetry breaking from isotropy.

The remainder of this note is divided into three sections. Section 2 discusses the basic structure of the continuum models of the visual cortex, the symmetries of these models, and some of the resulting cortical patterns. Section 3 outlines how Euclidean symmetry gives structure to the pattern

forming bifurcations by constraining the form of the possible eigenfunctions. Finally, in Section 4, we discuss the specific group actions and bifurcating branches of solutions that occur in symmetry-breaking bifurcations in the three different cortical models. We emphasize that the lists of solutions are model-independent; they depend on the way that Euclidean symmetry is present in the models and not on a specific set of differential equations.

## 2. Models, Symmetry, and Planforms

The Ermentrout and Cowan [10] model of V1 consists of neurons located at each point $\mathbf{x}$ in $\mathbf{R}^2$. Their model equations, variants of the Wilson-Cowan equations [23], are written in terms of a real-valued *activity variable* $a(\mathbf{x})$, where $a$ represents, say, the voltage potential of the neuron at location $\mathbf{x}$.

Bressloff *et al.* [5] incorporate the Hubel-Weisel hypercolumns [16] into their model of V1 by assuming that there is a hypercolumn centered at each location $\mathbf{x}$. Here a *hypercolumn* denotes a region of cortex that contains neurons sensitive to orientation $\varphi$ for each direction $\varphi$. Their models, also adaptations of the Wilson-Cowan equations [23], are written in terms of a real-valued *activity variable* $a(\mathbf{x}, \varphi)$ where $a$ represents, say, the voltage potential of the neuron tuned to orientation $\varphi$ in the hypercolumn centered at location $\mathbf{x}$. Note that angles $\varphi$ and $\varphi + \pi$ give the same orientation; so

$$a(\mathbf{x}, \varphi + \pi) = a(\mathbf{x}, \varphi).$$

The cortical planform associated to $a(\mathbf{x}, \varphi)$ is obtained in a way different from the Ermentrout-Cowan approach. For each fixed $\mathbf{x} \in \mathbf{R}^2$, $a(\mathbf{x}, \cdot)$ is a function on the circle. The planform associated to $a$ is obtained through a *winner-take-all* strategy. The neuron that is most active in its hypercolumn is presumed to suppress the activity of other neurons within that hypercolumn. The winner-take-all strategy chooses, for each $\mathbf{x}$, the directions $\varphi$ that maximize $a(\mathbf{x}, \cdot)$, and results in a field of directions. The two approaches to creating planforms can be combined by assigning directions only to those locations $\mathbf{x}$ where the associated maximum of $a(\mathbf{x}, \cdot)$ is larger than a given threshold. We will call these models the Ermentrout-Cowan model and the Wiener-Cowan model.

### *Euclidean Symmetry*

The Euclidean group $\mathbf{E}(2)$ is crucial to the analyses in both [10] and [5] — but the way that group acts is different. In Ermentrout-Cowan the Euclidean group acts on the plane by its standard action, whereas in Wiener-

Cowan the Euclidean group acts on $\mathbf{R}^2 \times \mathbf{S}^1$ by the so-called shift-twist representation, as we now explain.

Bressloff *et al.* [5] argue that the lateral connections between neurons in neighboring hypercolumns are anisotropic. *Anisotropy* means that the *strength* of the connections between neurons in two neighboring hypercolumns depends on the orientation tuning of both neurons and on the relative locations of the two hypercolumns. Anisotropy is idealized to the one illustrated in Figure 2 where only neurons with the same orientation selectivity are connected and then only neurons that are oriented along the direction of their cells preference are connected. In particular, the symmetries of V1 model equations are those that are consistent with the idealized structure shown in Figure 2.

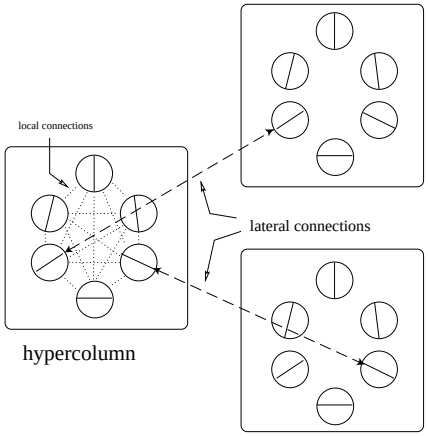


Fig. 2. Illustration of isotropic local and anisotropic lateral connection patterns.

The Euclidean group $\mathbf{E}(2)$ is generated by translations, rotations, and a reflection. The action of $\mathbf{E}(2)$ on $\mathbf{R}^2 \times \mathbf{S}^1$ that preserves the structure of lateral connections illustrated in Figure 2 is the *shift-twist* action. This action is given by:

$$\begin{aligned} \mathcal{T}_{\mathbf{y}}(\mathbf{x}, \varphi) &\equiv (\mathbf{x} + \mathbf{y}, \varphi) \\ \mathcal{R}_{\theta}(\mathbf{x}, \varphi) &\equiv (R_{\theta}\mathbf{x}, \varphi + \theta) \\ \mathcal{M}_{\kappa}(\mathbf{x}, \varphi) &\equiv (\kappa\mathbf{x}, -\varphi), \end{aligned} \tag{1}$$

where $(\mathbf{x}, \varphi) \in \mathbf{R}^2 \times \mathbf{S}^1$, $\mathbf{y} \in \mathbf{R}^2$, $\kappa$ is the reflection $(x_1, x_2) \mapsto (x_1, -x_2)$, and $R_{\theta} \in \mathbf{SO}(2)$ is rotation of the plane counterclockwise through angle $\theta$.

*Isotropy of Lateral Connections*

The anisotropy in lateral connections pictured in Figure 2 can be small in the sense that it is close to isotropic. We call the lateral connections between hypercolumns *isotropic*, as is done in Wolf and Geisel [24], if the strength of lateral connections between neurons in two neighboring hypercolumns depends only on the difference between the angles of the neurons' orientation sensitivity. Lateral connections in the isotropic model are illustrated in Figure 3. In this model, equations admit, in addition to Euclidean symmetry, the following $\mathbf{S}^1$ symmetry:

$$\mathcal{I}_{\widehat{\varphi}}(\mathbf{x}, \varphi) = (\mathbf{x}, \varphi + \widehat{\varphi}). \tag{2}$$

Note that $\widehat{\varphi} \in \mathbf{S}^1$ commutes with $\mathbf{y} \in \mathbf{R}^2$ and $R_\theta \in \mathbf{SO}(2)$, but $\kappa\widehat{\varphi} = (-\widehat{\varphi})\kappa$.

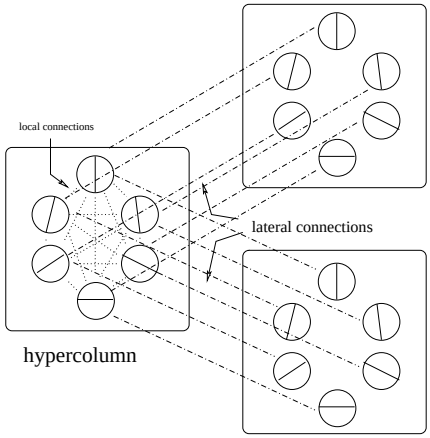


Fig. 3. Illustration of isotropic local and isotropic lateral connection patterns.

The action of $\gamma \in \mathbf{E}(2)\dot{+}\mathbf{S}^1$ on the activity function $a$ is given by

$$\gamma a(\mathbf{x}, \varphi) = a(\gamma^{-1}(\mathbf{x}, \varphi)).$$

For example, $R_\theta \in \mathbf{SO}(2)$ acts by

$$(\mathcal{R}_\theta a)(\mathbf{x}, \varphi) = a(R_{-\theta}\mathbf{x}, \varphi - \theta).$$

*Symmetry-Breaking Bifurcations on Lattices*

Spontaneous symmetry-breaking in the presence of a noncompact group such as the Euclidean group is far from understood. The standard approach

is to reduce the technical difficulties by looking only for solutions that are spatially doubly periodic with respect to some planar lattice (see Golubitsky and Stewart [14]); this is the approach taken in [5, 10, 13].

The first step in such an analysis is to choose a lattice type; in this paper we only describe transitions on square lattices. The second step is to decide on the size of the lattice. Euclidean symmetry guarantees that at bifurcation, critical eigenfunctions will have *plane wave* factors $e^{2\pi i \mathbf{k}\cdot\mathbf{x}}$ for some critical dual wave vector $\mathbf{k}$. See [4], Chapter 5 of [14], or Section 3. Typically, the lattice size is chosen so that the critical wave vectors will be vectors of shortest length in the dual lattice; that is, the lattice has the smallest possible size that can support doubly periodic solutions.

By restricting the bifurcation problem to a lattice, the group of symmetries is transformed to a compact group. First, translations in $\mathbf{E}(2)$ act modulo the spatial period as a 2-torus $\mathbf{T}^2$. Second, only those rotations and reflections in $\mathbf{E}(2)$ that preserve the lattice (namely, the holohedry $\mathbf{D}_4$ for the square lattice) are symmetries of the lattice restricted problem. Thus, the symmetry group of the square lattice problem is $\Gamma = \mathbf{D}_4 \dot{+} \mathbf{T}^2$. Recall that at bifurcation $\Gamma$ acts on the kernel of the linearization, and a subgroup of $\Gamma$ is *axial* if its fixed-point subspace in that kernel is one-dimensional. Solutions are guaranteed by the Equivariant Branching Lemma (see [14, 15]) which states: generically there are branches of equilibria to the nonlinear differential equation for every axial subgroup of $\Gamma$. The nonlinear analysis in [4, 10, 13] proceeds in this fashion.

*Previous Results on the Square Lattice*

In Ermentrout and Cowan [10] translation symmetry leads to eigenfunctions that are linear combinations of plane waves, and, on the square lattice, to two axial planforms: stripes and squares. See Figure 4.

In Bressloff *et al.* [4, 5] translation symmetry leads to critical eigenfunctions that are linear combinations of functions of the form $u(\varphi)e^{2\pi i \mathbf{k}\cdot\mathbf{x}}$. These eigenfunctions correspond to one of two types of representations of $\mathbf{E}(2)$ (restricted to the lattice): *scalar* ($u$ even in $\varphi$) and *pseudoscalar* ($u$ odd). The fact that two different representations of the Euclidean group can appear in bifurcations was first noted by Bosch Vivancos, Chossat, and Melbourne [2]. Bressloff *et al.* [5] also show that a trivial solution to the Wilson-Cowan equation will lose stability via a scalar or a pseudoscalar bifurcation depending on the exact form of the lateral coupling. Thus, each of these representations is, from a mathematical point of view, equally likely

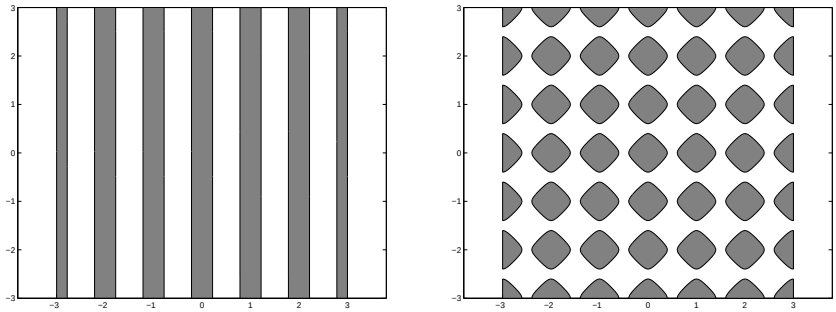

Fig. 4. Thresholding of eigenfunctions: (left) stripes, (right) squares.

to occur. On the square lattice, in [2,4] it is shown that there are two axial planforms each in the scalar and pseudoscalar cases: stripes and squares.

To picture the planforms in these cases, we must specify the function $u(\varphi)$, and this can be accomplished by assuming that anisotropy is small. When anisotropy is zero, the $\mathbf{S}^1$ symmetry in (2) forces $u(\varphi) = \cos(2m\varphi)$ in the scalar case and $u(\varphi) = \sin(2m\varphi)$ in the pseudoscalar case. (This point will be discussed in more detail when we review representation theory in Section 4.) The assumptions in Bressloff *et al.* [5] imply that $u$ is a small perturbation of sine or cosine. Note that the Ermentrout-Cowan planforms are recovered in the scalar case when $m = 0$ — in this case $u$ is constant and all directions are equally active. As often happens in single equation models, the first instability of a trivial (spatially constant) solution is to eigenfunctions with $m$ small — and that is what occurs in certain models based on the Wilson-Cowan equation (see [5]). Planforms for the scalar and pseudoscalar planforms when $m = 1$ are shown in Figure 5.

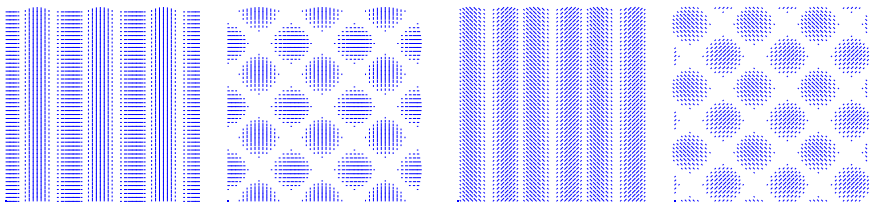


Fig. 5. Direction fields: scalar eigenfunctions (left) and pseudoscalar eigenfunctions (right)

*New Planforms When Lateral Connections are Isotropic*

In our analysis of the isotropic case ($\widetilde{\Gamma} = \Gamma \dot{+} \mathbf{S}^1$ symmetry) we find four axial subgroups ($\Sigma_1$-$\Sigma_4$) and one maximal isotropy subgroup $\Sigma_5$ with a two-dimensional fixed-point subspace. The axial subgroups lead to group orbits of equilibria. This fact must be properly interpreted to understand how the new planforms relate to the old. A phase shift of $\sin(2\varphi)$ yields $\cos(2\varphi)$. Thus, the extra $\mathbf{S}^1$ symmetry based on isotropic lateral connections identifies scalar and pseudoscalar planforms; up to this new symmetry the planforms are the same. Thus, the axial subgroup $\Sigma_3$ corresponds to stripes (both scalar and pseudoscalar) and the axial subgroup $\Sigma_1$ corresponds to squares (both scalar and pseudoscalar). The axial subgroups $\Sigma_2$ and $\Sigma_4$ correspond to new types of planforms. Finally, the maximal isotropy subgroup $\Sigma_5$ with its two-dimensional fixed-point subspace leads to a time-periodic rotating wave whose frequency is zero at bifurcation. The planforms associated with these new types of solutions are pictured in Figure 6.

It is unusual for a steady-state bifurcation (eigenvalues of a linearization moving through 0) to lead to time periodic states. It is well known that in systems without symmetry, time periodic states will appear in unfoldings of codimension two Takens-Bogdanov singularities (a double zero eigenvalue with a nilpotent normal form). It is less well known that codimension one steady-state bifurcations with symmetry can also lead to time periodic states. Field and Swift [11] were the first to find such a bifurcation (in a system with finite symmetry). Melbourne [19] was the first to find an example of a rotating wave in a steady-state bifurcation in a system with continuous symmetry. Nevertheless, the documented cases where time periodic states occur in codimension one steady-state bifurcations are relatively rare and our work provides the first example where this mathematical phenomenon appears in model equations.

*Weak Anisotropy in Lateral Connections*

Next, we discuss what happens to the bifurcating solutions to the isotropic nonlinear equation when anisotropy is added as a small symmetry-breaking parameter. As was noted in Bressloff *et al.* [5], the linear effect of anisotropy is to split the eigenfunctions into scalar and pseudoscalar representations. The effect on solutions to the nonlinear equation can also be established using the methods of Lauterbach and Roberts [18]. This method is applied independently to each branch of (group orbits of) solutions found in the

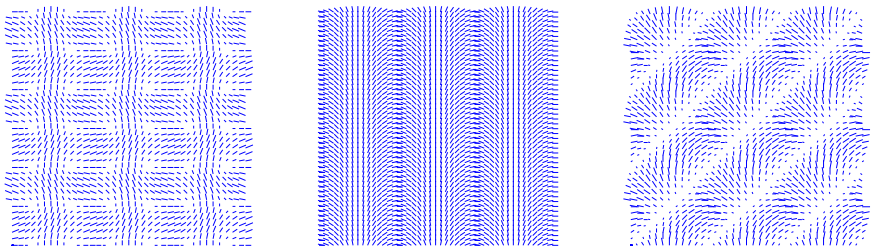

Fig. 6. Direction fields of new planforms in isotropic model: (left) axial planform $\Sigma_2$; (center) axial planform $\Sigma_4$; (right) rotating wave $\Sigma_5$ (direction of movement is up and to the left).

isotropic case. The results for square lattice solutions are easily described.

Generically, the dynamics on the $\widetilde{\Gamma}$ group orbit of equilibria corresponding to the axial subgroup $\Sigma_3$ has two (smaller) $\Gamma$ group orbits of equilibria: scalar stripes and pseudoscalar stripes. There may be other equilibria coming from the $\widetilde{\Gamma}$ group orbit; but at the very least scalar and pseudoscalar stripes always remain as solutions.

Similarly, the dynamics on the group orbit of equilibria corresponding to the axial subgroup $\Sigma_1$ generically have two equilibria corresponding to scalar and pseudoscalar squares.

The dynamics on the group orbit of the axial subgroups $\Sigma_2$ and $\Sigma_4$ and the fifth maximal isotropy subgroup $\Sigma_5$ do not change substantially when anisotropy is added. These group orbits still remain as equilibria and rotating waves.

*Retinal Images*

Finally, we discuss the geometric form of the cortical planforms in the visual field, that is, we try to picture the corresponding visual hallucinations. It is known that the density of neurons in the visual cortex is uniform, whereas the density of neurons in the retina fall offs from the fovea[c] at a rate of $1/r^2$. Schwartz [22] observed that there is a unique conformal map taking a disk with $1/r^2$ density to a rectangle with uniform density, namely, the complex logarithm. This is also called the *retino-cortical* map. It is thought that using the inverse of the retino-cortical map, the complex exponential, to push forward the activity pattern from V1 to the retina is a reasonable way to form the hallucination image — and this is the approach

[c]The *fovea* is the small central area of the retina that gives the sharpest vision.

used in Ermentrout and Cowan [10] and in Bressloff *et al.* [5,6]. Specifically, the transformation from polar coordinates $(r, \theta)$ on the retina to cortical coordinates $(x, y)$ is given in Cowan [9] to be:

$$\begin{aligned} x &= \tfrac{1}{\varepsilon} \ln \left(\tfrac{1}{\omega} r\right) \\ y &= \tfrac{1}{\varepsilon} \theta \end{aligned} \tag{3}$$

where $\omega$ and $\varepsilon$ are constants. See Bressloff *et al.* [6] for a discussion of the values of these constants. The inverse of the retino-cortical map (3) is

$$\begin{aligned} r &= \omega \exp(\varepsilon x) \\ \theta &= \varepsilon y \end{aligned} \tag{4}$$

In our retinal images we take

$$\omega = \frac{30}{e^{2\pi}} \quad \text{and} \quad \varepsilon = \frac{2\pi}{n_h}$$

where $n_h$ is the number of hypercolumn widths in the cortex, which we take to be 36.

The images of these cortical patterns in retinal coordinates, as well as the discussion of additional issues concerning the construction of these images, are given in [13].

## 3. A Brief Outline of Local Equivariant Steady-State Bifurcation Theory

In finite dimensions steady-state bifurcation reduces to finding all zeros of a parameterized map $f : \mathbf{R}^n \times \mathbf{R} \to \mathbf{R}^n$ near a known zero, which we can take to be $f(0, 0) = 0$. In equivariant bifurcation theory we assume that $f$ commutes with the action of a compact Lie group $\Gamma$, that is, $\Gamma \subset \mathbf{O}(n)$ and

$$f(\gamma x, \lambda) = \gamma f(x, \lambda) \tag{5}$$

for all $\gamma \in \Gamma$ and that $f$ has a *trivial* $\Gamma$-invariant solution for all $\lambda$, that is, $f(0, \lambda) = 0$. It follows from (5) and the chain rule that the Jacobian at a trivial solution also commutes with $\Gamma$, that is,

$$(df)_{0,\lambda} \gamma = \gamma (df)_{0,\lambda} \tag{6}$$

for all $\gamma \in \Gamma$.

A steady-state bifurcation occurs at $\lambda = 0$ when $\mathcal{K} \equiv \ker L \neq 0$, where $L = (df)_{0,0}$. It follows from (6) that $\mathcal{K}$ is $\Gamma$-invariant. Indeed, generically $\mathcal{K}$ is an (absolutely) irreducible representation of $\Gamma$. Liapunov-Schmidt and center manifold reductions can be performed in a way that preserves symmetry. In either case, finding the zeros of $f$ reduces to finding the zeros of

a map $g : \mathcal{K} \times \mathbf{R} \to \mathcal{K}$ near the trivial solution $g(0, \lambda) = 0$. Moreover, $g$ commutes with the action of $\Gamma$ on the kernel $\mathcal{K}$ and $(dg)_{0,0} = 0$.

In general $\mathcal{K}$ can still be a large dimensional space and finding the zeros of $g$ can be a daunting task. However, the Equivariant Branching Lemma [14,15] enables one to find many (though not all) of the zeros of $g$. This lemma states that generically for each axial subgroup $\Sigma$ of the action of $\Gamma$ on $\mathcal{K}$, there exists a unique (local) branch of zeros of $g$ whose solutions have $\Sigma$ symmetry. An *axial* subgroup is an isotropy subgroup whose fixed-point subspace

$$\mathrm{Fix}(\Sigma) = \{x \in \mathcal{K} : \sigma x = x \quad \forall \sigma \in \Sigma\}$$

is one-dimensional.

It is important to note that the existence of axial solutions is *model independent*. The existence of axial solutions does not depend (in any essential way) on $f$ — just on the form of the action of $\Gamma$ on $\mathcal{K}$. Detailed statements and proofs can be found in Chapter 1 of [14].

### *Euclidean Symmetry and Eigenfunctions*

Planar pattern formation arguments begin by assuming that a uniform (Euclidean invariant) equilibrium for a Euclidean equivariant system of differential equations loses stability as a parameter is varied. For hallucination models we assume that the system of differential equations is defined on the space $\mathbf{R}^2 \times \Omega$ where $\Omega$ is a point in the Ermentrout-Cowan model and $\Omega = \mathbf{S}^1$ in the orientation tuning models. More precisely, the system of (partial) differential equations should be viewed as an operator $f$ on the space of real-valued functions $\mathcal{F}$ defined on $\mathbf{R}^2 \times \Omega$.

There is a fundamental complication that appears when trying to apply the outline of equivariant steady-state bifurcation theory to planar pattern formation: $\mathcal{K}$ need not be finite-dimensional. To understand this difficulty, and one way around it, we next discuss how Euclidean symmetry determines the eigenfunctions of $L$.

Let $\mathbf{k} \in \mathbf{R}^2$ and let

$$W_{\mathbf{k}} = \{u(\varphi)e^{i\mathbf{k}\cdot\mathbf{x}} + \text{c.c.} : u : \Omega \to \mathbf{C}\}$$

Observe that translations act on $W_{\mathbf{k}}$ by

$$T_{\mathbf{y}}(u(\varphi)e^{i\mathbf{k}\cdot\mathbf{x}}) = u(\varphi)e^{i\mathbf{k}\cdot(\mathbf{x}+\mathbf{y})} = \left[e^{i\mathbf{k}\cdot\mathbf{y}}u(\varphi)\right]e^{i\mathbf{k}\cdot\mathbf{x}}$$

It follows that $L : W_{\mathbf{k}} \to W_{\mathbf{k}}$ and that eigenfunctions of $L$ have *plane wave* factors. The vectors $\mathbf{k}$ are called *dual wave vectors*.

Let $\rho$ be the reflection such that $\rho\mathbf{k} = \mathbf{k}$. Euclidean equivariance implies

$$\rho\left(u(\varphi)e^{i\mathbf{k}\cdot\mathbf{x}}\right) = \rho(u(\varphi))e^{i\mathbf{k}\cdot\mathbf{x}}$$

So $\rho : W_{\mathbf{k}} \to W_{\mathbf{k}}$. It follows from $\rho^2 = 1$ that

$$W_{\mathbf{k}} = W_{\mathbf{k}}^+ \oplus W_{\mathbf{k}}^-$$

where $\rho$ acts as $+1$ on $W_{\mathbf{k}}^+$ and $-1$ on $W_{\mathbf{k}}^-$. Hence, eigenfunctions of $L$ are either even ($W_{\mathbf{k}}^+$) or odd ($W_{\mathbf{k}}^-$). When $\mathbf{k} = (1, 0)$

$$u(-\varphi) = \begin{cases} u(\varphi) & u \in W_{\mathbf{k}}^+ \\ -u(\varphi) & u \in W_{\mathbf{k}}^- \end{cases}$$

Finally, rotations act on the subspaces $W_{\mathbf{k}}$ by

$$R_\theta\left(u(\varphi)e^{i\mathbf{k}\cdot\mathbf{x}}\right) = R_\theta(u(\varphi))e^{iR_\theta(\mathbf{k})\cdot\mathbf{x}}$$

Therefore

$$R_\theta(W_{\mathbf{k}}) = W_{R_\theta(\mathbf{k})}$$

Hence, for each eigenfunction in $W_{\mathbf{k}}$, there is an independent eigenfunction in $W_{R_\theta(\mathbf{k})}$ and $\ker L$ is $\infty$-dimensional. Standard reductions theorems then fail.

### *Euclidean Equivariant Bifurcation Theory*

A standard way around this difficulty is to look for solutions in the space of double-periodic functions. Let $\mathcal{L}$ be a planar lattice and let

$$\mathcal{F}_{\mathcal{L}} = \{a : \mathbf{R}^2 \times \Omega \to \mathbf{R} : a(\mathbf{x} + \boldsymbol{\ell}, \varphi) = h(\mathbf{x}, \varphi) \quad \forall \boldsymbol{\ell} \in \mathcal{L}\}$$

There are only a finite number of rotations that leave $\ker(L|\mathcal{F}_{\mathcal{L}})$ invariant, namely, the rotations that preserve the lattice $\mathcal{L}$. Thus, $\ker(L|\mathcal{F}_{\mathcal{L}})$ is generically finite-dimensional and we can choose the size of the lattice so that the shortest dual wave vectors $\mathbf{k}$ are the critical eigenvectors.

Note that the symmetries that act on the function space $\mathcal{F}_{\mathcal{L}}$ are different from those that act on the base space $\mathbf{R}^2 \times \Omega$ in two ways: translations act on $\mathcal{F}_{\mathcal{L}}$ as a 2-torus $\mathbf{T}^2$ and only those rotations and reflections that preserve the lattice $\mathcal{L}$ (often called the *holohedry* subgroup $H$) act on $\mathcal{F}_{\mathcal{L}}$. Thus the group of symmetries acting on the reduction to doubly-periodic states is the compact group $H\dot{+}\mathbf{T}^2$. For square lattices $H = \mathbf{D}_4$ and for hexagonal lattices $H = \mathbf{D}_6$. We report here on the simpler square lattice case. The symmetry group for the Ermentrout-Cowan model and the anisotropic model is $\Gamma = \mathbf{D}_4\dot{+}\mathbf{T}^2$; the symmetry group for the isotropic model is $\widetilde{\Gamma} = \Gamma\dot{+}\mathbf{S}^1$.

## 4. Square Lattice Planforms

In this section we discuss the spatially doubly periodic solutions that must emanate from the simplest bifurcations of Euclidean invariant differential equations restricted to a square lattice. To do this we describe the simplest kernel $\mathcal{K}$, the representations of $\Gamma$ and $\widetilde{\Gamma}$ on $\mathcal{K}$, and the axial subgroups of these actions.

### 4.1. *Representation Theory of* $\Gamma$ *and* $\widetilde{\Gamma}$

Without loss of generality, we assume that the square lattice $\mathcal{L}$ consists of squares of unit length. The action of $\widetilde{\Gamma}$ on $\mathcal{F}_{\mathcal{L}}$ is the one induced from the action of $\mathbf{E}(2)\dot{+}\mathbf{S}^1$ on $\mathbf{R}^2 \times \mathbf{S}^1$ given in (1) and (2).

We expect the simplest square lattice bifurcations to be from equilibria whose linearizations have kernels that are irreducible subspaces of $\mathcal{F}_{\mathcal{L}}$ and we only consider bifurcations based on dual wave vectors of shortest (unit) length. We write $\mathbf{x} = (x_1, x_2)$.

The eigenfunctions corresponding to $\Gamma$ in the Ermentrout-Cowan models have the form

$$a(\mathbf{x}) = z_1 e^{2\pi i x_1} + z_2 e^{2\pi i x_2} + c.c.$$

where $(z_1, z_2) \in \mathbf{C}^2$.

The eigenfunctions corresponding to $\Gamma$ in the Wiener-Cowan models have the form

$$a(\mathbf{x}, \varphi) = z_1 u(\varphi) e^{2\pi i x_1} + z_2 u(\varphi - \frac{\pi}{2}) e^{2\pi i x_2} + c.c.$$

where $(z_1, z_2) \in \mathbb{C}^2$ and $u(\varphi)$ is $\pi$-periodic, real-valued, and either odd or even. See [4].

The eigenfunctions corresponding to $\widetilde{\Gamma}$ have the form

$$\begin{aligned} a(\mathbf{x}, \varphi) = &\left(z_1 e^{2i\varphi} + w_1 e^{-2i\varphi}\right) e^{2\pi i \mathbf{k}_1 \cdot \mathbf{x}} + \\ &\left(z_2 e^{2i(\varphi - \pi/2)} + w_2 e^{-2i(\varphi - \pi/2)}\right) e^{2\pi i \mathbf{k}_2 \cdot \mathbf{x}} + c.c. \end{aligned} \tag{7}$$

where $(z_1, w_1, z_2, w_2) \in \mathbf{C}^4$. See [13].

### 4.2. *Group Actions on* $\mathcal{K}$ *and their Axial Subgroups*

A calculation shows that the actions of $\Gamma$ on $\mathbf{C}^2$ (in the scalar and pseudoscalar representations) and of $\widetilde{\Gamma}$ on $\mathbf{C}^4$ (when $m = 1$) are as given in Table 1.1.

Table 1.1. For Ermentrout-Cowan and for $u(\varphi)$ even, let $\varepsilon = +1$; for $u(\varphi)$ odd, let $\varepsilon = -1$.

| $\mathbf{D}_4$ | Action on $\mathbf{C}^2$ | Isotropic Case Action on $\mathbf{C}^4$ |
|---|---|---|
| $\mathbf{1}$ | $(z_1, z_2)$ | $(z_1, w_1, z_2, w_2)$ |
| $\xi$ | $(\overline{z_2}, z_1)$ | $(\overline{w}_2, \overline{z}_2, z_1, w_1)$ |
| $\xi^2$ | $(\overline{z_1}, \overline{z_2})$ | $(\overline{w}_1, \overline{z}_1, \overline{w}_2, \overline{z}_2)$ |
| $\xi^3$ | $(z_2, \overline{z_1})$ | $(z_2, w_2, \overline{w}_1, \overline{z}_1)$ |
| $\kappa$ | $\varepsilon(z_1, \overline{z_2})$ | $(w_1, z_1, \overline{z}_2, \overline{w}_2)$ |
| $\kappa\xi$ | $\varepsilon(\overline{z_2}, \overline{z_1})$ | $(\overline{z}_2, \overline{w}_2, \overline{z}_1, \overline{w}_1)$ |
| $\kappa\xi^2$ | $\varepsilon(\overline{z_1}, z_2)$ | $(\overline{z}_1, \overline{w}_1, w_2, z_2)$ |
| $\kappa\xi^3$ | $\varepsilon(z_2, z_1)$ | $(w_2, z_2, w_1, z_1)$ |
| $[\theta_1, \theta_2]$ | $(e^{-2\pi i\theta_1} z_1, e^{-2\pi i\theta_2} z_2)$ | $(e^{2\pi i\theta_1} z_1, e^{2\pi i\theta_1} w_1, e^{2\pi i\theta_2} z_2, e^{2\pi i\theta_2} w_2)$ |
| $[0, 0, \widehat{\varphi}]$ | | $(e^{-2i\varphi} z_1, e^{2i\varphi} w_1, e^{-2i\varphi} z_2, e^{2i\varphi} w_2)$ |

The axial subgroups of $\Gamma$ acting on $\mathbf{C}^2$ are given in Table 1.2 and the maximal isotropy subgroups of $\widetilde{\Gamma}$ acting on $\mathbf{C}^4$ are given in Table 1.3. Observe that the action of $\widetilde{\Gamma}$ on $W_1$ has four axial subgroups $\Sigma_1$-$\Sigma_4$ and one maximal isotropy subgroup with a two-dimensional fixed-point subspace $\Sigma_5$.

Table 1.2. Square lattice axial subgroups of $\Gamma$ acting on $\mathbf{C}^2$.

| $\varepsilon = +1$ | $\varepsilon = -1$ | Fixed Subspace |
|---|---|---|
| $\Sigma_1 = \langle \xi, \kappa \rangle$ | $\langle \xi, \kappa[\frac{1}{2}, \frac{1}{2}] \rangle$ | $\mathbf{R}\{(1,1)\}$ |
| $\Sigma_2 = \langle \xi^2, \kappa, [0, \theta_2] \rangle$ | $\langle \xi^2, \kappa[\frac{1}{2}, 0], [0, \theta_2] \rangle$ | $\mathbf{R}\{(1,0)\}$ |

Table 1.3. Square lattice maximal isotropy subgroups of $\widetilde{\Gamma}$ acting on $\mathbf{C}^4$; $u \in \mathbf{C}$.

| Isotropic case | Fixed Subspace |
|---|---|
| $\Sigma_1 = \langle \kappa, \xi \rangle$ | $\mathbf{R}\{(1,1,1,1)\}$ |
| $\Sigma_2 = \langle \kappa, [\frac{3}{4}, \frac{1}{4}, \frac{\pi}{4}]\, \xi \rangle$ | $\mathbf{R}\{(1,1,1,-1)\}$ |
| $\Sigma_3 = \langle \kappa, \xi^2, [0, \theta_2, 0] \rangle$ | $\mathbf{R}\{(1,1,0,0)\}$ |
| $\Sigma_4 = \langle \kappa\xi^2, [0, \theta_2, 0], [\theta_1, 0, \pi\theta_1] \rangle$ | $\mathbf{R}\{(1,0,0,0)\}$ |
| $\Sigma_5 = \langle \kappa\xi, [\theta_1, \theta_1, \pi\theta_1] \rangle$ | $\{(u, 0, \overline{u}, 0)\}$ |

**The Effect of Weak Anisotropy** We discuss how solutions corresponding to $\widetilde{\Gamma}$-bifurcations behave generically when the isotropy of the lateral connections is broken, that is, when the $\widetilde{\Gamma}$-equivariant vector field is perturbed to a $\Gamma$-equivariant field. Detailed arguments in [13] show that equilibria corresponding to the axial subgroups $\Sigma_1 - \Sigma_4$ persist on symmetry-breaking perturbations. More interesting, the maximal isotropy subgroup $\Sigma_5$ with a

two-dimensional fixed-point subspace in the isotropic case leads to circles of equilibria and to periodic solutions on the breaking of $\widetilde{\Gamma}$ symmetry to $\Gamma$ symmetry. Moreover the period of this periodic solution tends to $\infty$ at the bifurcation point ($\lambda = 0$).

**Concluding Remarks** We note that pattern formation on the hexagonal lattice is also treated in [5,6,13]. The calculations are more difficult and the results more complicated but the basic ideas are the same. Note that tunnelling and pulsating periodic solutions occur only on a hexagonal lattice. We expect pseudoscalar representations, as well as the usual scalar representations to occur in a variety of pattern formation problems, particularly those where the pattern produces a line-field rather than just a threshold or level contour. Another example occurs in liquid crystals; see [7].

***Acknowledgements***

We are grateful to Jack Cowan, Paul Bressloff, and Peter Thomas for many helpful conversations about the delightful structure of and pattern formation on the visual cortex. This work was supported in part by NSF Grant DMS-0244529.

## References

[1] G.G. Blasdel. *J. Neurosci.* **12** (1992) 3139–3161.
[2] I. Bosch Vivancos, P. Chossat, and I. Melbourne, *Arch. Rational Mech. Anal.* **131** (1995) 199–224.
[3] W.H. Bosking, Y. Zhang, B. Schofield, and D. Fitzpatrick, *J. Neurosci.* **17** 6 (1997) 2112–2127.
[4] P.C. Bressloff, J.D. Cowan, M. Golubitsky, and P.J. Thomas, *Nonlinearity* **14** (2001) 739–775.
[5] P.C. Bressloff, J.D. Cowan, M. Golubitsky, P.J. Thomas, and M.C. Wiener, *Phil. Trans. Royal Soc. London* ***B*** **356** (2001) 299–330.
[6] P.C. Bressloff, J.D. Cowan, M. Golubitsky, P.J. Thomas and M.C. Wiener, *Neural Computation* **14** (2002) 473–491.
[7] D. Chillingworth and M. Golubitsky, *J. Math. Phys.* **44** (9) (2003) 4201–4219.
[8] J. Clottes and D. Lewis-Williams. *The Shamans of Prehistory: Trance and Magic in the Painted Caves*. Abrams, New York, 1998.
[9] J.D. Cowan, *Neurosciences Research Program Bull.*, **15** (1977) 492–517.
[10] G.B. Ermentrout and J.D. Cowan, *Biol. Cybernetics* **34** (1979) 137–150.
[11] M. Field and J.W. Swift, *Nonlinearity* **4** (1991) 1001–1043.
[12] C.D. Gilbert, *Neuron* **9** (1992) 1–13.

[13] M. Golubitsky, L-J. Shiau and A. Török, *SIAM J. Appl. Dynam. Sys.* **2** (2003) 97–143.
[14] M. Golubitsky and I. Stewart. *The Symmetry Perspective: From Equilibrium to Chaos in Phase Space and Physical Space*, Progress in Mathematics **200**, Birkhäuser, Basel, 2002.
[15] M. Golubitsky, I.N. Stewart and D.G. Schaeffer. *Singularities and Groups in Bifurcation Theory: Vol. II*, Applied Mathematical Sciences **69**, Springer-Verlag, New York, 1988.
[16] D.H. Hubel and T.N. Wiesel, *J. Comp. Neurol.* **158** No. 3 (1974) 267–294; *J. Comp. Neurol.* **158** No. 3 (1974) 295–306; *J. Comp. Neurol.* **158** No. 3 (1974) 307–318.
[17] H. Klüver. *Mescal and Mechanisms of Hallucinations*. University of Chicago Press, Chicago, 1966.
[18] R. Lauterbach and M. Roberts, *J. Diff. Eq.* **100** (1992) 22–48.
[19] I. Melbourne, *Nonlinearity* **7** (1994) 1385–1393.
[20] A. Patterson. *Rock Art Symbols of the Greater Southwest*. Johnson Books, Boulder, 1992.
[21] G. Oster, *Scientific American* **222** No. 2 (1970) 83–87.
[22] E. Schwartz, *Biol. Cybernetics* **25** (1977) 181–194.
[23] H.R. Wilson and J.D. Cowan, *Biophys. J.* (1972) **12** 1–24.
[24] F. Wolf and T. Geisel,*Nature* **395** (1998) 73–78.